Hexagonal-close-packed lattice: Ground state and phase transition

Danh-Tai Hoang* and H. T. Diep†
Laboratoire de Physique Théorique et Modélisation, Université de Cergy-Pontoise, CNRS, UMR 8089 and 2, Avenue Adolphe Chauvin, F-95302 Cergy-Pontoise Cedex, France
(Received 24 December 2011; published 9 April 2012)

We study the ground state (GS) and the phase transition in a hexagonal-close-packed lattice with both *XY* and Ising models by using extensive Monte Carlo simulation. We suppose the in-plane interaction J_1 and interplane interaction J_2, both antiferromagnetic. The system is frustrated with two kinds of GS configuration below and above a critical value of $\eta = J_1/J_2$ (η_c). For the Ising case, one has $\eta_c = 0.5$ which separates in-plane ferromagnetic and antiferromagnetic states, while for the *XY* case $\eta_c = 1/3$ separates the collinear and noncollinear spin configurations. The phase transition is shown to be of first (second) order for $\eta > (<)\eta_c$. The phase diagram in the space (η,T) is shown for both cases.

DOI: 10.1103/PhysRevE.85.041107 PACS number(s): 05.70.Fh, 75.10.Hk, 75.40.Mg, 75.47.−m

I. INTRODUCTION

Frustrated spin systems have been the subject of intensive investigations during the last 30 years [1]. These systems are very unstable due to the competition between antagonist interactions or due to a geometrical frustration such as in the antiferromagnetic (AF) triangular lattice. A spin is said frustrated when it cannot find an orientation which "fully" satisfies all the interactions with its neighbors [2,3]. As a consequence of the frustration, the ground state (GS) is very highly degenerate. In the Ising case the GS degeneracy is often infinite as in the triangular lattice, the face-centered cubic (FCC), and hexagonal-close-packed (HCP) lattices, with AF interaction. In the case of vector spins, the GS is noncollinear such as the 120° configuration in the *XY* and Heisenberg AF stacked triangular lattice (STL). In two dimensions (2D), several frustrated systems with the Ising spin model have been exactly solved [4,5]. Among the most interesting models one can mention the frustrated generalized Kagome lattice [6] and the honeycomb lattice [7] where exotic features such as the existence of several phase transitions, the reentrance, and the disorder lines have been exactly found by mapping these systems into vertex models [8]. In three dimensions (3D), the situation is complicated. The renormalization group (RG) [9,10], which provided a good understanding of the nature of the phase transition in nonfrustrated systems, encounters much of the difficulties in application to frustrated systems. Among the most studied subjects during the last 20 years, one can mention the nature of the phase transition in the *XY* and Heisenberg STL. After a long debate [11] on whether it is a second-, or a first-order transition or it belongs to a new universality class, the controversy has recently ended with the conclusion of a first-order transition: Let us mention the work of Itakura who, using Monte Carlo (MC) and MC RG, has early identified a first-order behavior in the *XY* STL case [12], the work of Bekhechi *et al.* [13] who, using a short-time critical dynamics, have led to the same conclusion, and finally the works of Ngo and Diep who put an end to the controversy [14,15].

In this paper, we are interested in the HCP antiferromagnet with Ising and *XY* spin models. Our purpose is to study its properties such as the ground state and the phase transition, in the case of anisotropic exchange interactions. The isotropic nearest-neighbor (NN) AF interaction has been studied for Ising [16] and *XY* and Heisenberg spins [17]. These isotropic cases have been shown to undergo a phase transition of first order, and the infinite GS degeneracy is reduced to 6 at low temperatures [16,17]. The effect of anisotropic interaction and anisotropy on the GS in the case of vector spins has been studied [18].

In Sec. II, we show our model and analyze the ground state. Results of MC simulations on the phase transition are shown and discussed in Sec. III. Concluding remarks are given in Sec. IV.

II. MODEL AND GROUND-STATE ANALYSIS

We consider the HCP lattice shown in Fig. 1. The stacking direction is z. The Hamiltonian is given by

$$\mathcal{H} = -\sum_{(i,j)} J_{i,j}\mathbf{S}_i \cdot \mathbf{S}_j, \tag{1}$$

where $\mathbf{S}_i$ is the spin at lattice site i and J_{ij} is the AF interaction between nearest neighbors (NN). We suppose that $J_{ij} = J_1$ if the NN are on the xy triangular plane, and $J_{ij} = J_2$ if the NN are on two adjacent planes (see Fig. 1). The GS can be determined by the steepest-descent method. This method is very simple [19]. (i) We generate an initial configuration at random, (ii) we calculate the local field created at a site by its neighbors using (1), (iii) we align the spin of that site along the calculated local field to minimize its energy, (iv) we go to another site and repeat until all sites are visited: we say we make one sweep, and (v) we do a large number of sweeps per site until a good convergence is reached.

However, one can also minimize the interaction energy as shown below to calculate the GS configuration. Since both interactions are AF (negative), for simplicity, we fix $J_2 = -1$ and vary J_1. The unit of energy is taken as $|J_2|$ and the temperature T is in the unit of $|J_2|/k_B$ where k_B is the Boltzmann constant.

*danh-tai.hoang@u-cergy.fr
†Corresponding Author: diep@u-cergy.fr

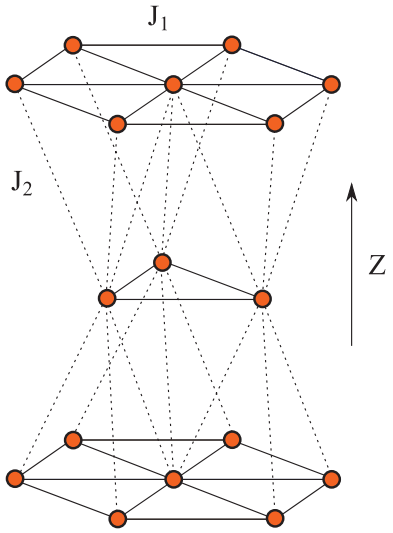

FIG. 1. (Color online) HCP lattice. The in-plane and interplane interactions are indicated by J_1 and J_2.

Let us recall the GS in the case of isotropic interaction, namely, $J_1 = J_2$ [17]. For the HCP lattice, each spin is shared by eight tetrahedra (four in the upper half-space and four in the lower half-space along the z axis) and an NN bond is shared by two tetrahedra. The GS spin configuration of the system is formed by stacking neighboring tetrahedra. In the GS, one has two pairs of antiparallel spins on each tetrahedron. Their axes form an arbitrary angle α. The degeneracy is thus infinite [see Fig. 2(a) of Ref. [17]]. Of course, the periodic boundary conditions will reduce a number of configurations, but the degeneracy is still infinite. Of these GS's, one particular family of configurations of interest for both *XY* and Heisenberg cases is when $\alpha = 0$. The GS is then collinear with two spins up and the other two down. The stacking sequence is then simplest: there are three equivalent configurations since there are three ways to choose the parallel spin pair in the original tetrahedron.

We now examine the case where $J_1 \neq J_2$:

(1) *Ising case*. The steepest descent method with varying J_1 ($J_2 = -1$) gives two kinds of GS spin configuration: The first consists of xy ferromagnetic planes stacked antiferromagnetically along the z direction, while the second one is the stacking of xy AF planes such that each tetrahedron has two up and two down spins. The transition between the two configurations is determined as follows. One simply writes down the respective energies of a tetrahedron and compares them:

$$E_1 = 3(-J_1 + J_2), \tag{2}$$

$$E_2 = J_1 + J_2. \tag{3}$$

One sees that $E_1 < E_2$ when $J_1 > 0.5J_2$, that is, $|J_1| < 0.5|J_2|$. Thus the first configuration is more stable when $|J_1| < 0.5|J_2|$.

(2) *XY case*. Consider one tetrahedron of the HCP lattice. The Hamiltonian for this cell is given by

$$\begin{aligned}\mathcal{H}_c = &-J_1(\mathbf{S}_1\cdot\mathbf{S}_2 + \mathbf{S}_2\cdot\mathbf{S}_3 + \mathbf{S}_3\cdot\mathbf{S}_1)\\ &-J_2(\mathbf{S}_1\cdot\mathbf{S}_4 + \mathbf{S}_2\cdot\mathbf{S}_4 + \mathbf{S}_3\cdot\mathbf{S}_4).\end{aligned} \tag{4}$$

Suppose that $|\mathbf{S}_i| = 1$, one has

$$\begin{aligned}\mathcal{H}_c = &-J_1[\cos\alpha + \cos\beta + \cos(\alpha+\beta)]\\ &-J_2[\cos\gamma + \cos(\gamma-\alpha) + \cos(\gamma-\alpha-\beta)],\end{aligned} \tag{5}$$

where the angles are defined in Fig. 2. The steepest descent method shows that while β and α have unique values for a

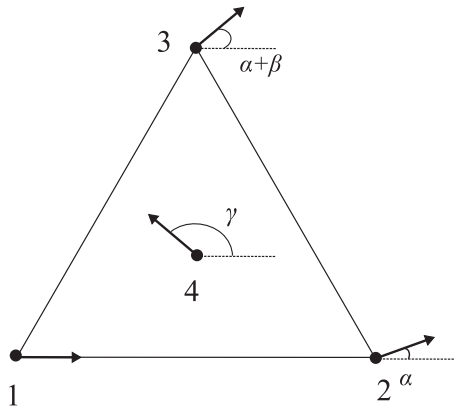

FIG. 2. Ground state in the *XY* case. The tetrahedron is projected on the xy plane. The spins are numbered from 1 to 4. See text for comments.

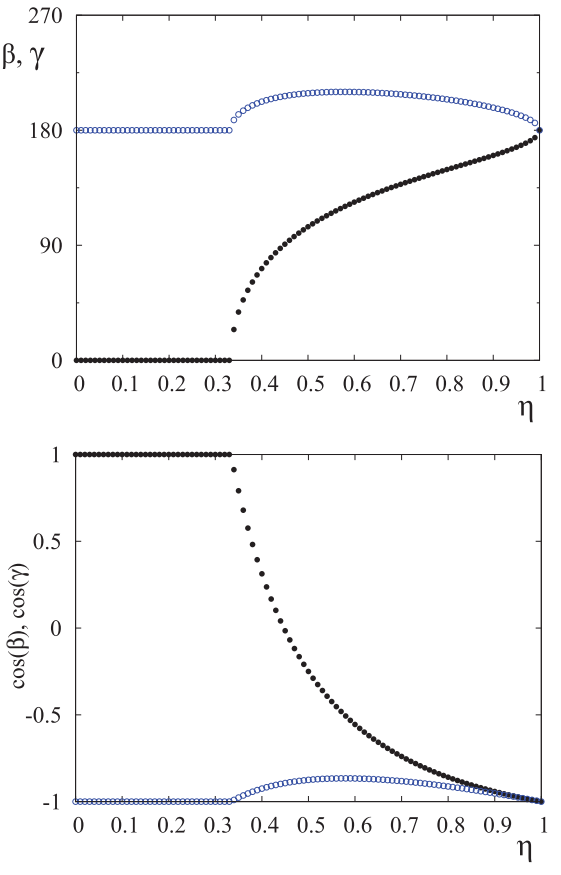

FIG. 3. (Color online) Ground state in the *XY* case (color online). The angles β (black circles) and γ (blue void circles) and their cosinus are shown as functions of $\eta = J_1/J_2$. Noncollinear GS configurations occur in the region $1/3 \leqslant \eta \leqslant 1$. See text for comments.

given J_1/J_2, α is arbitrary, just as in the case of the isotropic interaction [17] discussed above. To simplify the formulas, we take $\alpha = 0$ in the following. The energy of the cell is written as

$$\mathcal{H}_c = -J_1[1 + 2\cos\beta] - J_2[2\cos\gamma + \cos(\gamma - \beta)]. \quad (6)$$

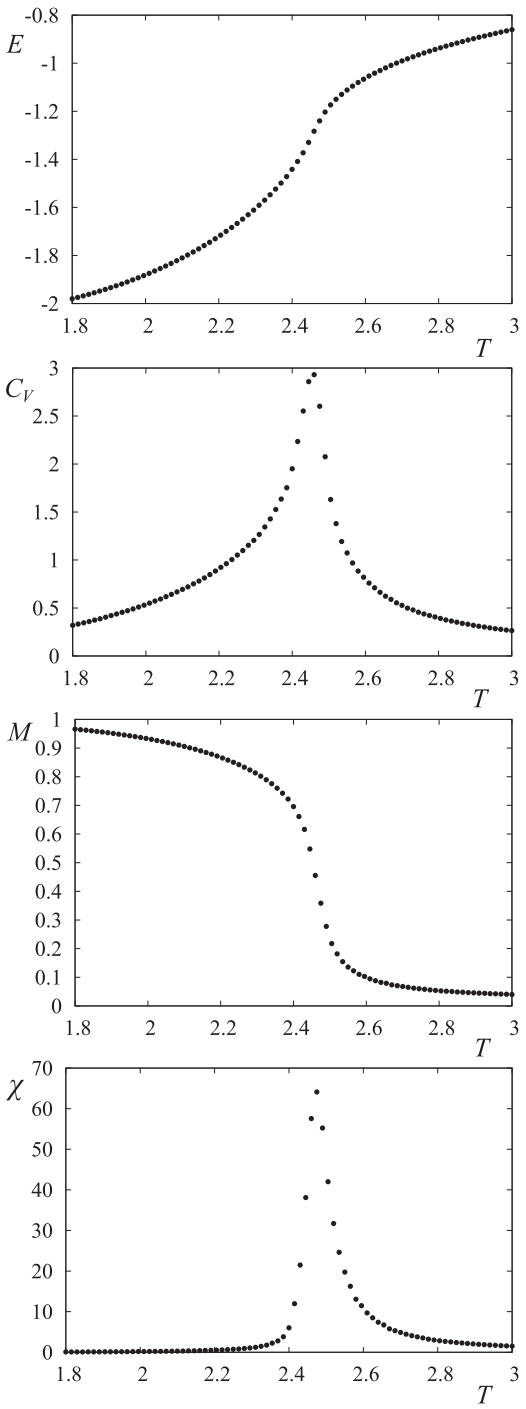

FIG. 4. Ising case. Energy E, specific heat C_V, order parameter M, and susceptibility χ versus T for $\eta = J_1/J_2 = 0.3$. See text for comments.

The critical values of β and γ are determined from the relations,

$$\frac{\partial \mathcal{H}_c}{\partial \beta} = 2J_1 \sin\beta - 2J_2 \sin(\gamma - \beta) = 0, \quad (7)$$

$$\frac{\partial \mathcal{H}_c}{\partial \gamma} = 2J_2 \sin\gamma + J_2 \sin(\gamma - \beta) = 0. \quad (8)$$

We find the following solutions:
(i) $\beta = 0, \gamma = 0$,
(ii) $\beta = 0, \gamma = \pi$,
(iii) $\beta = \pi, \gamma = 0$,
(iv) $\beta = \pi, \gamma = \pi$, and
(v) $\cos\beta = \frac{1}{4(J_1/J_2)^2} - \frac{5}{4}$, $\cos\gamma = -\frac{1+3(J_1/J_2)^2}{4(J_1/J_2)}$.
By comparing the energy values at these solutions, we obtain the minimum energy with the last solution: One has

$$\mathcal{H}_c = -\frac{1 + 3(J_1/J_2)^2}{2(J_1/J_2)}, \quad (9)$$

where $\cos\beta$ and $\cos\gamma$ are given above.
Because $-1 \leqslant \cos\beta \leqslant 1$ and $-1 \leqslant \cos\gamma \leqslant 1$, the above solution is valid for $\frac{1}{3} \leqslant J_1/J_2 \leqslant 1$. We plot $\cos\beta$, $\cos\gamma$, β, and γ in Fig. 3 where we observe that the noncollinear GS configuration occurs in the interval $1/3 \leqslant \eta = J_1/J_2 \leqslant 1$.

III. PHASE TRANSITION: RESULTS

We consider a sample size of $L \times L \times L_z$ where L and L_z vary from 12 to 36 but L_z can be different from L in order to detect the dependence of the GS on J_1. The exchange interaction $|J_2| = 1$ is used as the unit of energy. We use

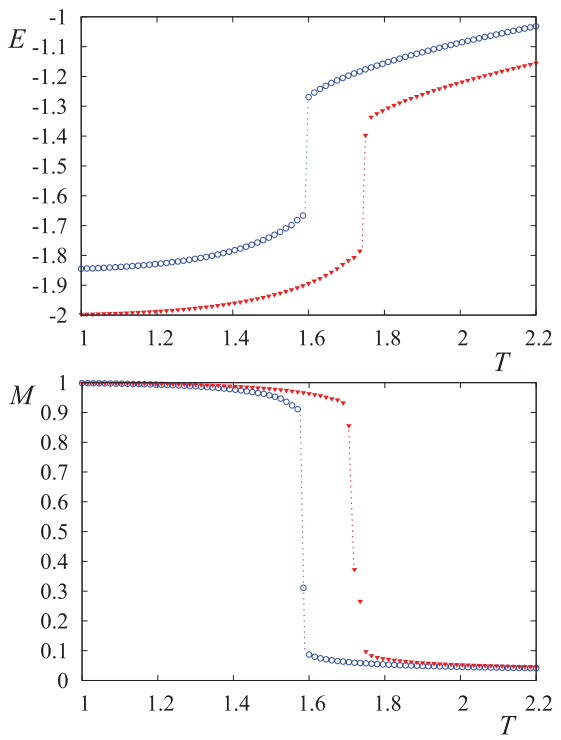

FIG. 5. (Color online) Ising case. Energy E and order parameter M for $\eta = J_1/J_2 = 0.85$ (blue open circles) and 1 (red triangles). See text for comments.

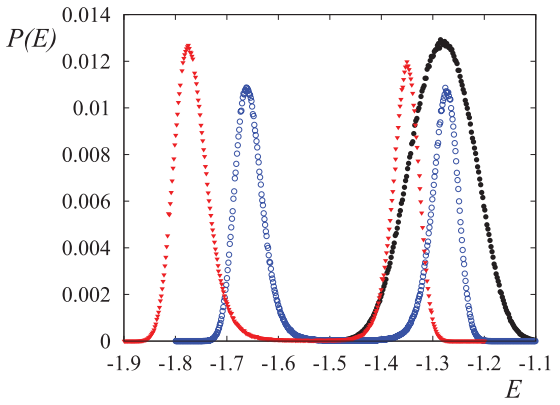

FIG. 6. (Color online) Ising case. Energy histogram $P(E)$ versus E for $\eta = 1$(red triangles), 0.85 (blue open circles), and 0.3 (black circles). See text for comments.

here MC simulations with a histogram technique to detect first-order transition. We equilibrate the system and average physical quantities over several millions of MC steps per spin. The averaged energy $\langle U \rangle$ and the heat capacity C_V are calculated by

$$\langle U \rangle = \langle \mathcal{H} \rangle, \tag{10}$$

$$C_V = \frac{\langle U^2 \rangle - \langle U \rangle^2}{k_B T^2}, \tag{11}$$

where $\langle \cdots \rangle$ indicates the thermal average taken over microscopic states at T.

The order parameter M is defined from the sublattice magnetization by

$$M = \sum_K \left| \sum_{i \in K} \mathbf{S}_i \right|, \tag{12}$$

where $\mathbf{S}_i$ belongs to the sublattice K. Note that there are at least four sublattices which define the ordering of the spins on the tetrahedra if a long-range order is observed. The susceptibility

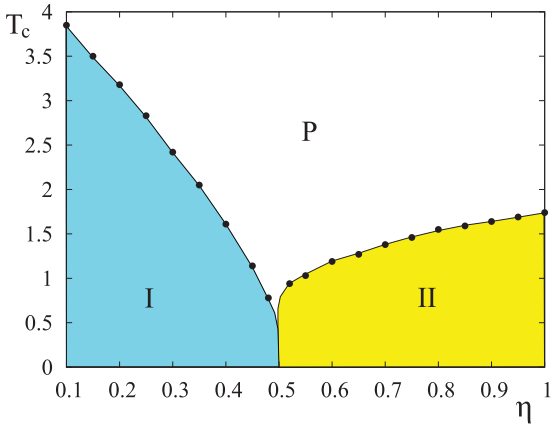

FIG. 7. (Color online) Ising case. T_C versus η. I, II, and P denote the first, second, and paramagnetic phases, respectively. See text for comments.

is defined by

$$\chi = \frac{\langle M^2 \rangle - \langle M \rangle^2}{k_B T}. \tag{13}$$

In MC simulations, we work at finite sizes, so for each size we have to determine the "pseudo" transition which corresponds in general to the maximum of the specific heat or of the susceptibility. The maxima of these quantities need not be at the same temperature. Only at the infinite size, they should coincide. The theory of finite-size scaling [20–22] permits

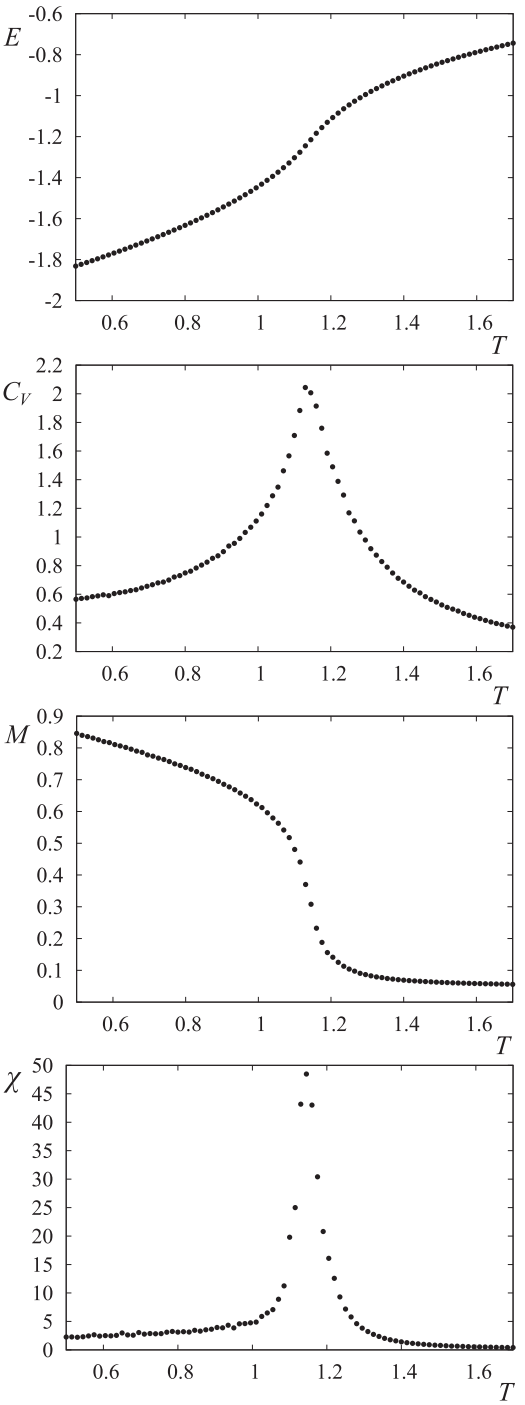

FIG. 8. XY case. Energy E, specific heat C_V, order parameter M, and susceptibility χ versus T for $\eta = 0.3$. See text for comments.

one to deduce properties of a system at its thermodynamic limit. In order to check the first-order nature of the transition, we used the histogram technique which is very efficient in detecting weak first-order transitions and in calculating critical exponents of second-order transitions [21,22]. The main idea of this technique is to make an energy histogram at a temperature T_0 as close as possible to the transition temperature. Often, one has to try at several temperatures in the transition region. Using this histogram in the formulas of statistical physics for canonical distribution, one obtains energy histograms in a range of temperature around T_0. In second-order transitions, these histograms are Gaussian. This allows us to calculate averages of physical quantities as well as critical exponents using the finite-size scaling. In first-order transitions, the energy histogram shows a double-peak structure.

A. Ising case

In the following, the results in different figures are shown with $L = 18$ and $L_z = 8$ (16 atomic planes along z). Since the GS changes at $\eta_c = 0.5$, we show here examples on both sides of this value. Figure 4 shows the energy per spin E, the specific heat per spin C_V, the order parameter M, and the susceptibility χ, for $\eta = 0.3$. The transition is of second order. On the other side, we show in Fig. 5 the energy per spin and the order parameter versus T, for $\eta = 0.85$ and 1. We find a strong first-order transition in both cases. The discontinuity of E and M at the transition is very large. We show in Fig. 6 the energy histogram taken at the transition temperature for three values $\eta = 0.3$ (black), 0.85 (blue), and 1 (red). As seen,

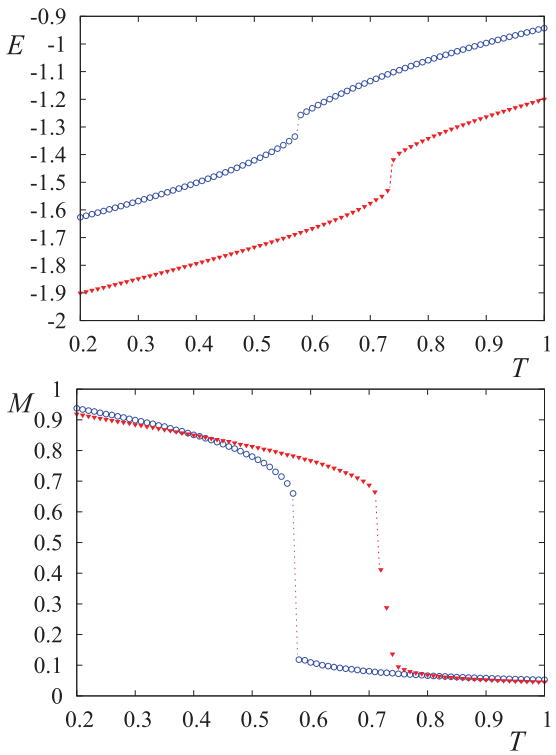

FIG. 9. (Color online) *XY* case. E and M versus T for $\eta = 0.58$ (blue open circles) and 1 (red triangles). See text for comments.

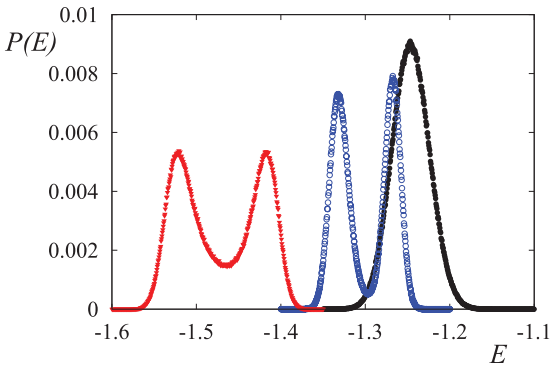

FIG. 10. (Color online) *XY* case. Energy histogram P versus E for $\eta = 0.3$ (black circles), 0.58 (blue open circles), and 1 (red triangles) at the respective transition temperatures. See text for comments.

the first case is a Gaussian distribution indicating a second-order transition, while the last two cases show a double-peak structure indicating a first-order transition.

We have calculated the critical temperature T_C as a function of η. The phase diagram is shown in Fig. 7 where I and II indicate the ordering of the first and second kinds, respectively. P indicates the paramagnetic phase. Note that the transition line between I and P is a second-order line, while that between II and P is a first-order line.

B. *XY* case

In the *XY* case, the change of the GS takes place at $\eta = 1/3$. Let us show in Fig. 8 the result for $\eta = 0.3$ where the GS is composed of ferromagnetic planes antiferromagnetically stacked in the z direction. The transition is of second order.

We show now the result for the noncollinear GS region in Fig. 9. The energy and the order parameter show clearly a discontinuity at the transition for $\eta = 0.58$ and 1. Using the histogram method described above, we have calculated the histogram shown in Fig. 10 for $\eta = 0.3$, 0.58, and 1. For $\eta = 0.3$ which is in the collinear region of the GS, the histogram is Gaussian, confirming the second-order transition observed in the data shown above. For $\eta = 0.58$ and 1 belonging to the

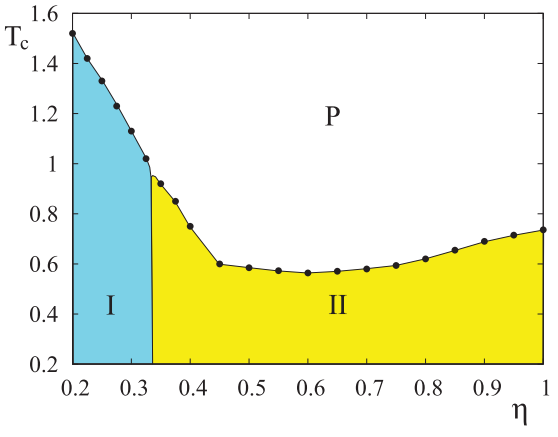

FIG. 11. (Color online) *XY* case. T_C versus η. I, II, and P denote the collinear, noncollinear, and paramagnetic phases, respectively. See text for comments.

noncollinear region, the histogram shows a two-peak structure which confirms the first-order character of the transitions in this region.

The two peaks are very well separated with the dip going down to zero, indicating an energy discontinuity. The distance between the two peaks is the latent heat ΔE.

We show in Fig. 11 the transition temperature versus η where I and II indicate the collinear and noncollinear phases, respectively. P denotes the paramagnetic state. The line separating I and P is a second-order transition line, while that separating II and P is the first-order one.

To close this section, we emphasize that all three-dimensional (3D) frustrated systems known so far undergo a first-order transition: Let us mention the AF STL [12–15], the FCC antiferromagnets [23], the simple cubic fully frustrated lattices [24–27], helimagnets [28], and the HCP lattice studied here.

IV. CONCLUSION

We have studied in this paper some properties of the HCP antiferromagnet with Ising and XY spin models. The in-plane J_1 and interplane J_2 interactions are supposed to be different. As a result, the GS spin configuration depends on the ratio $\eta = J_1/J_2$. We show that there exists a critical value η_c where the GS changes. For the Ising case, we find $\eta_c = 0.5$ below (above) which the spins in the xy planes are ferromagnetic (antiferromagnetic). For the XY case, the GS is collinear below $\eta_c = 1/3$, and is noncollinear above that value. The nature of the transition changes from a second order below η_c to a first order above η_c for both Ising and XY cases. The general phase diagrams in the space (η, T) are shown for both cases. These findings may help to understand the transition nature in different compounds with HCP structure.

[1] H. T. Diep (ed.), *Frustrated Spin Systems* (World Scientific, Singapore, 2005).
[2] G. Toulouse, Commun. Phys. **2**, 115 (1977).
[3] J. Villain, J. Phys. C **10**, 1717 (1977).
[4] R. Liebmann, *Statistical Mechanics of Periodic Frustrated Ising Systems*, Lecture Notes in Physics Vol. 251 (Springer-Verlag, Berlin, 1986).
[5] H. T. Diep and H. Giacomini, in *Frustrated Spin Systems* (World Scientific, Singapore, 2005), pp. 1-57.
[6] M. Debauche, H. T. Diep, P. Azaria, and H. Giacomini, Phys. Rev. B **44**, 2369 (1991).
[7] H. T. Diep, M. Debauche, and H. Giacomini, Phys. Rev. B **43**, R8759 (1991).
[8] R. J. Baxter, *Exactly Solved Models in Statistical Physics* (Academic Press, London, 1982).
[9] K. G. Wilson, Phys. Rev. B **4**, 3174 (1971).
[10] J. Zinn-Justin, *Quantum Field Theory and Critical Phenomena*, 4th ed. (Oxford University Press, Oxford, 2002); D. J. Amit, *Field Theory, the Renormalization Group and Critical Phenomena* (World Scientific, Singapore, 1984).
[11] B. Delamotte, D. Mouhanna, and M. Tissier in *Frustrated Spin Systems* (World Scientific, Singapore, 2005), pp. 107-171.
[12] M. Itakura, J. Phys. Soc. Jpn. **72**, 74 (2003).
[13] S. Bekhechi, B. W. Southern, A. Peles, and D. Mouhanna, Phys. Rev. E **74**, 016109 (2006).
[14] V. Thanh Ngo and H. T. Diep, J. Appl. Phys. **103**, 07C712 (2008).
[15] V. T. Ngo and H. T. Diep, Phys. Rev. E **78**, 031119 (2008).
[16] D. Auerbach, E. Domany, and J. E. Gubernatis, Phys. Rev. B **37**, 1719 (1988).
[17] H. T. Diep, Phys. Rev. B **45**, 2863 (1992).
[18] B. E. Larson, J. Appl. Phys. **67**, 5240 (1990).
[19] V. T. Ngo and H. T. Diep, Phys. Rev. B **75**, 035412 (2007).
[20] P. C. Hohenberg and B. I. Halperin, Rev. Mod. Phys. **49**, 435 (1977).
[21] A. M. Ferrenberg and R. H. Swendsen, Phys. Rev. Lett. **61**, 2635 (1988); **63**, 1195 (1989).
[22] A. M. Ferrenberg and D. P. Landau, Phys. Rev. B **44**, 5081 (1991).
[23] H. T. Diep and H. Kawamura, Phys. Rev. B **40**, 7019 (1989).
[24] D. Blankschtein, M. Ma, and A. N. Berker, Phys. Rev. B **30**, 1362 (1984).
[25] V. T. Ngo, D. T. Hoang, and H. T. Diep, Phys. Rev. E **82**, 041123 (2010).
[26] V. Thanh Ngo, D. Tien Hoang, and H. T. Diep, Mod. Phys. Lett. B **25**, 929 (2011).
[27] V. Thanh Ngo, D. Tien Hoang, and H. T. Diep, J. Phys.: Condens. Matter **23**, 226002 (2011).
[28] H. T. Diep, Phys. Rev. B **39**, 397 (1989).